

Chapter 36

Analysis of Aluminum AA6061 in Electromagnetic Forming



Nilesh Tiwari and Megha Nagrale

Abstract Weight reduction in the automotive and aerospace industries is of special importance. This leads to lower fuel consumption and high efficiency. Discharge circuit parameters and mechanical properties vary during the electromagnetic forming process. The mechanical properties change along with time and tube length during the electromagnetic expansion. A coupled analytical model is developed to predict the parametric variation of the discharge circuit, corresponding radial pressure and stress acting on the tube. The electromagnetic forming simulation was performed on 2.5 mm thick aluminum tube with a length of 100 mm using 7 turns helical copper coil. A 2D coupled simulation model is developed using COMSOL MULTIPHYSICS software and simulation results are used to compare with analytical results. Based on which maximum deformation is predicted during the electromagnetic forming process and work-piece hardness is obtained.

Keywords Electromagnetic forming · High strain rate · Plastic deformation · Lorentz' force

Nomenclature

EMF	Electromagnetic forming
$I(t)$	Current at that instant (A)
$U(t)$	Charging voltage (V)
$E_c(t)$	Stored energy in the capacitor (KJ)
ω	Frequency of the current (Hz)
β	Damping coefficient
v	Velocity of the tube at a point (m/sec)
d	Displacement of the tube (mm)

N. Tiwari (✉) · M. Nagrale
Department of Mechanical Engineering, Sardar Patel College of Engineering,
Mumbai 400 058, India
e-mail: ntiwari252@gmail.com

© Springer Nature Singapore Pte Ltd. 2020
V. S. Sharma et al. (eds.), *Manufacturing Engineering*,
Lecture Notes on Multidisciplinary Industrial Engineering,
https://doi.org/10.1007/978-981-15-4619-8_36

36.1 Introduction

Due to low density, high strength to weight ratio aluminum alloy is increasingly focused on and widely applied fields such as automotive, aerospace industry which craves the lightweight designs to enhance fuel utilization and reduce the cost of production [1]. Electromagnetic forming is an impulse or high-speed forming technology which uses a pulse magnetic field to apply Lorentz' force on the work-piece made up of highly electrically conductive material without mechanical contact or working medium. In the electromagnetic forming process, it can shape and weld similar or dissimilar metal along with other benefits (e.g., high precision, short cycle time, uniform strain distribution). The main components of the electromagnetic forming process are high voltage power supply, capacitor bank, switch (trigger), and forming coil. In the electromagnetic forming process, a capacitor bank charges with a significant amount of electrical energy at constant current and then discharges the coil quickly. The energy is dissipated in a coil is in damped form because of the presence of resistance and inductance in coil and tube. A high-intensity magnetic field is generated which induces an eddy current in nearby conductive materials tube [2]. This eddy current produces a repulsive field called Lorentz forces which deform the work-piece plastically when magnetic pressure exceeds the flow stress of work-piece.

When the work-piece starts deforming due to magnetic pressure, the gap between the coil and work-piece increases which causes two opposite effects, First, the flux density between the coil and the work-piece gets reduced and the magnetic force decreases because magnetic pressure is proportional to magnetic flux density. Secondly, due to the plastic deformation of work-piece strain hardening takes place due to which more force is required to deform further [3].

In a loose coupling simulation approach, magnetic pressure and solid mechanics physics are solved separately. This approach doesn't consider the work-piece deformation on the magnetic force or discharge circuit parameters. In the sequentially coupled simulation approach, both the magnetic and solid mechanics are used to solve sequentially and the feedback of work-piece displacement is taken into account to calculate the magnetic pressure at every step. When high energy is applied, more deformation occurs due to which gap increases between the tube and coil. This effect is not considered in the loose coupling due to which more errors occur in the loosely coupled approach compared to sequential coupling approach [4].

36.2 Analytical Approach

Figure 36.1 represents the systematic arrangement of tube and coil and the system specification is shown in Table 36.1. To accelerate the tube, internally the gap of 0.5–2 mm is provided between work-piece and coil.

As tube deforms the gap between the coil and tube increases due to which the resistance and inductance of system increase which is calculated by the author Dond

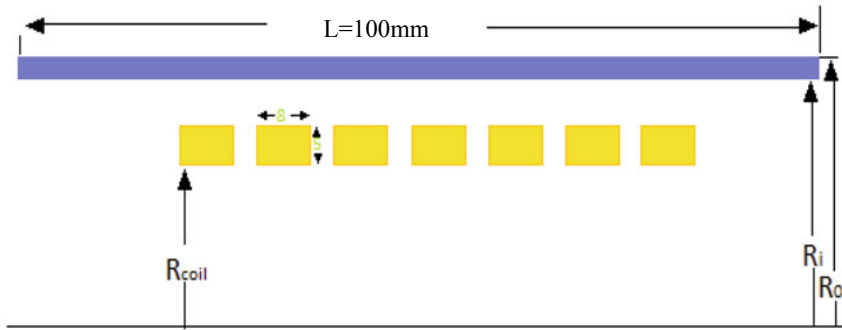


Fig. 36.1 Cross-section of coil and tube (work-piece) in the EMF process

Table 36.1 System specification

R_{system}	L_{system}	C_{system}	Coil c/s	R_{coil}	R_i	Thickness
14.83 mΩ	1.3 μH	112 μF	8 × 5 mm	16.5 mm	25 mm	2.5 mm

[3]. In the case of COMSOL software both physics (solid mechanics and magnetics) are used to solve the simulations simultaneously such that after resistance iteration the inductance changes. Therefore, only the initial numerical value is used for software analysis.

36.2.1 Analytical Approach to Find Flow Stress of the Material

When the strain rates increase, the mechanical property of materials changes. The variation in material strength with applied strain rate is an important consideration in the design of classes of materials used in structures subjected to suddenly applied loads. It has been observed that for many materials the stress is found to increase rapidly with strain rate for a given suddenly applied load (Fig. 36.2).

To evaluate the constitutive response of the materials the flow stress is determined as a function of plastic strain, strain rate and the temperature induced during the model, to evaluate the flow stress using Johnson–cook model[J-C] [5].

$$\sigma = (A + B(\epsilon^n)) \left(1 + c \ln \left(\frac{\dot{\epsilon}}{\dot{\epsilon}_0} \right) \right) \left(1 - \left(\frac{T - T_{room}}{T_{melt} - T_{room}} \right) \right) \quad (36.1)$$

In the electromagnetic forming process only work-piece is deformed and hence the temperature induced is very less which can be neglected. In the case of magnetic pulse welding, impact between tube and block causes temperature rise that is calculated

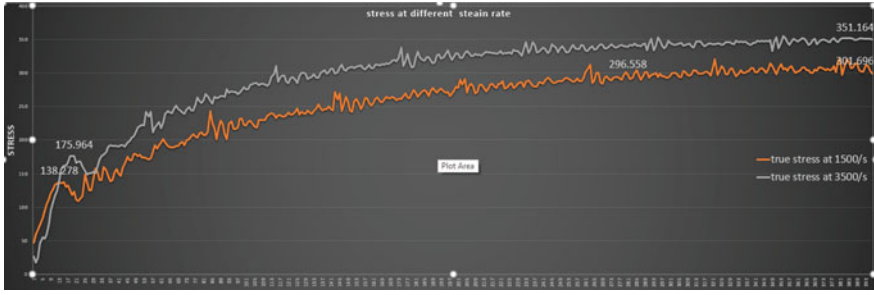


Fig. 36.2 Stress versus strain at different strain rate

by using a joule effect.

$$Q = J^2 \rho_r \tag{36.2}$$

- Q Heat generated per unit volume (W/m^3)
- J Current density in (A/m^2)
- ε Equivalent plastic strain
- $\dot{\varepsilon}$ Equivalent plastic strain rate
- ε_0 Reference plastic strain

In Eq. (36.1), parameter A represents the initial yield strength of the material at room temperature where B , C , N and M are constant which is determined by stress and strain curve.

In the present work, work-piece of aluminum alloy (AA6061) has been used as a tube for calculation. The constitutive parameter required by the Johnson–cook constitutive model is shown in Table 36.2 for aluminum alloy [6].

Table 36.2 Johnson–cook model for aluminum alloy (AA6061)

Density (ρ)	2700 kg/m^3	A	110 MPA
Modulus of rigidity (G)	26 GPA	B	114 MPA
Modulus of elasticity (E)	68.9 GPA	C	0.002
Poisson’s ratio (ν)	0.31	N	0.42
Heat capacity (C)	896 $\text{J}/\text{Kg}\cdot\text{K}$	T_m	925 K
Thermal conductivity (k)	167 $\text{W}/\text{m}\cdot\text{k}$	M	1.34
Electrical conductivity (σ)	25 MS/m	T_{room}	298 K

36.3 Experimental Setup

36.3.1 Materials

In Table 36.3 for material compositions and their constituents are shown. Work-piece is made of aluminum and coil made of copper.

Figure 36.3 shows the setup of an electromagnetic forming configuration that corresponds to a resonant circuit.

A constant current source used to charge the capacitor through switch 1 at a certain level of energy which energy discharge into a coil in the form of a pulse. A pulse generator achieves the high magnetic field that is necessary for forming of work-piece having high electrical conductivity. The coil and work-piece units are characterized as transformer [7].

The forming machine is represented by a series circuit consisting of a capacitor C , an inductance L_i as well as resistor R_i . Resistance R_{coil} and inductance L_{coil} both are connected in series to the pulse power generator represent the tool coil as shown in Fig. 36.4. To analysis the process EMF circuit to equivalent circuit.

In the electromagnetic forming process, the capacitor charges up to the desired energy level $E_c(t)$.

Through the constant current, according to Eq. (36.3), energy can be calculated by multiplication of the capacity C and the charging voltage $U(t)$ and rapidly discharged

Table 36.3 Material composition

Material (%wt)	Si	Fe	Cu	Mn	Mg	Cr	Ti	Al
AA6061	0.6	0.58	0.202	0.042	0.741	0.207	0.052	Bal.
Coil materials	00	00	99	0.06	0.56	0.07	0.31	00

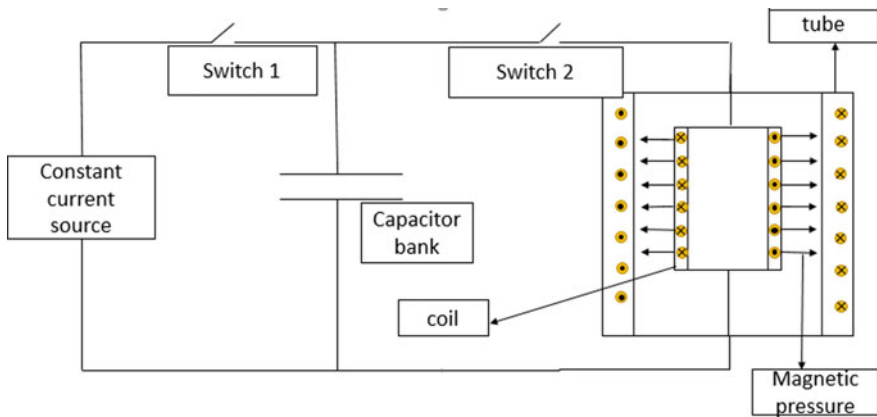


Fig. 36.3 Schematic of the EMF system

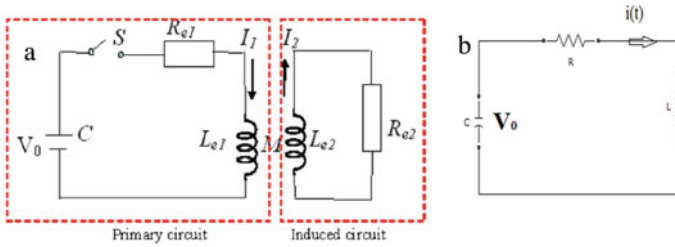


Fig. 36.4 Equivalent circuit diagram a Detailed version b Reduced version [7]

into the coil by closing switch (trigger).

$$E_c(t) = \frac{1}{2}CU(t)^2 \tag{36.3}$$

The resulting current $I(t)$ is a damped sinusoidal oscillation which is determined by the electrical property of the resonant circuit. For the calculation purpose, all parameters of EMF are converted into a single parameter that is the inductance of the system, inductance of coil and inductance of tube into equivalent inductance.

From the Fig. 36.4b,

$$I(t) = \frac{U(t)}{S(R + LS + \frac{1}{CS})} \tag{36.4}$$

After solving the equation, we get the damped sinusoidal current waveform, i.e.,

$$I(t) = \frac{U(t)}{\omega L}e^{-\beta t} \sin(\omega t) \tag{35.5}$$

where

Damping coefficient (β) $\frac{R}{2L}$
 The Frequency of current (ω) $\sqrt{\frac{1}{LC} - \beta^2}$

The current is related to the corresponding magnetic field which is concentrated between the work-piece and the tool coil. This magnetic field creates an eddy current that flows in the opposite direction in the work-piece. These are located close to the surface of the work-piece due to skin depth effect. The depth of penetration of the current into the work-piece is called skin depth (δ), where

- μ_0 Magnetic permeability in vacuum
- f Represents the frequency of discharge current.

$$\delta = \sqrt{\frac{1}{\pi f k \mu_0}} \quad (36.6)$$

The volume force \vec{F} acting on work-piece can be determined based on the current density \vec{J} and the magnetic flux density \vec{B} :

$$\begin{aligned} \vec{F} &= \vec{J} \times \vec{B} \\ \vec{J} &= -\frac{\partial H}{\partial r} \end{aligned} \quad (36.7)$$

$$\begin{aligned} \vec{B} &= \mu \times H \\ F_r &= \frac{1}{2} \mu \frac{\partial H^2}{\partial r} \end{aligned} \quad (36.8)$$

The volume force acting on the work-piece can be transformed mathematically to the virtual surface that called magnetic pressure (p) for that apply surface integral to convert volumetric force into surface pressure [8].

$$P(r, t) = \int_{r_o}^{r_i} F(r, t) dr = \frac{1}{2} \mu H_{\text{gap}}^2(t) \quad (36.9)$$

$$\begin{aligned} H(t) &= \frac{N * I(t)}{l} \\ P &= \mu \left(\frac{N U(t)}{l \omega L} \right)^2 e^{-2\beta t} (1 - \cos(2\omega t)) \end{aligned} \quad (36.10)$$

Figure 36.5 show that the actual pressure acting on the tube that decreases with time, when tube deforms, its stress increases but for simplicity take as constant.

The Lorentz force is used as an input to the mechanical model. In the solid mechanics to solve 3-D stress problem used compatibility equation. Due to axis-symmetric, the problem reduced to a 1-D problem as shown in Eq. (36.11).

$$\rho \frac{\partial^2 u}{\partial t^2} - \nabla \cdot \sigma_s = \vec{F} \quad (36.11)$$

$$a = \frac{p}{\rho * s} - \frac{\sigma * S * r i(t)}{r i * \rho * r i} \quad (36.12)$$

$$v = \int_0^t a * dt \quad (36.13)$$

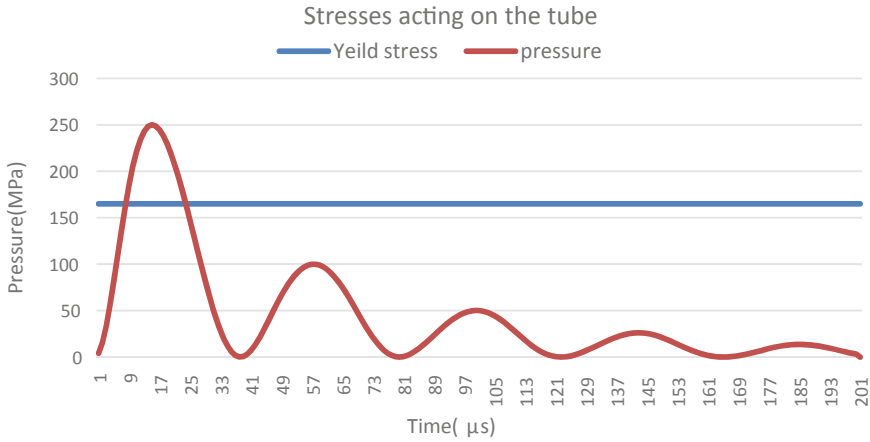


Fig. 36.5 Stress acting on the tube during the EMF process

$$dis = \int_0^t v * dt \tag{36.14}$$

The forming process is completed within 200 μs . In this process up to 500 MPa pressure is applied in an extremely short time. When the stress exceeds the flow stress work-piece due to magnetic pressure it deforms plastically. In 200 μs only up to 50 μs force is effective after which pressure decreases below the yield stress. The yield stress depends on the strain rate, which is calculated by Johnson–cook model.

As shown in Fig. 36.6 displacement of tube during when the pressure acting on the with respect to time. First 50 μs deformation takes place by magnetic pressure

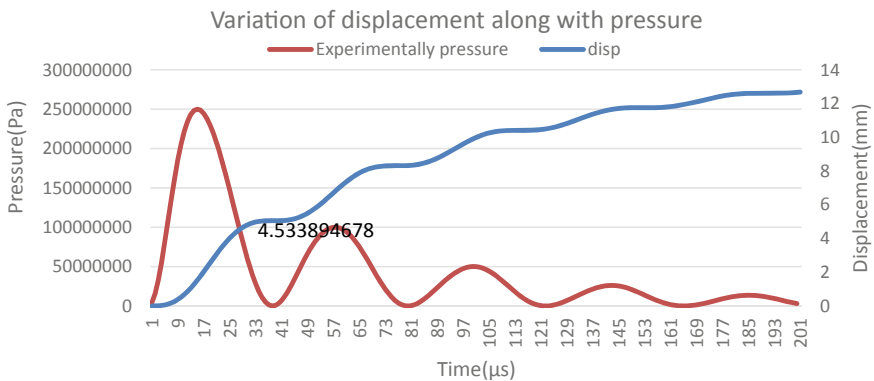


Fig. 36.6 Displacement variation with respect to pressure

after which deformation takes place because of inertia of tube. In the first 50 μ s inertia oppose the deformation after which it helps in the deformation of work-piece.

36.3.2 Simulation Approach

As shown in Fig. 36.7. It consists of seven turns helical copper coil having dimensions of 8×5 mm and its length 47 mm and place an aluminum tube having length 100 mm in front of copper coil. For the experiment, the tube of outer diameter 55 mm is used. After completing drawing as per specification next is to add material like copper to coil and aluminum to tube and also air for surrounding tube and coil. After adding materials add physics which is used to analyze in EMF process for this add magnetic field and solid mechanics. After adding physics apply the boundary conditions after which apply type of study, i.e., time-dependent. After adding the type of study, mesh the model. Meshing is important because if meshing is coarse then results are approximate, if mesh is fine then it gives accurate results but time-consuming hence optimize the mesh. In EMF, mesh size is from 0.1 to 1 mm after which results are not accurate because the gap between tube and coil varies from 1 to 2.5 mm.

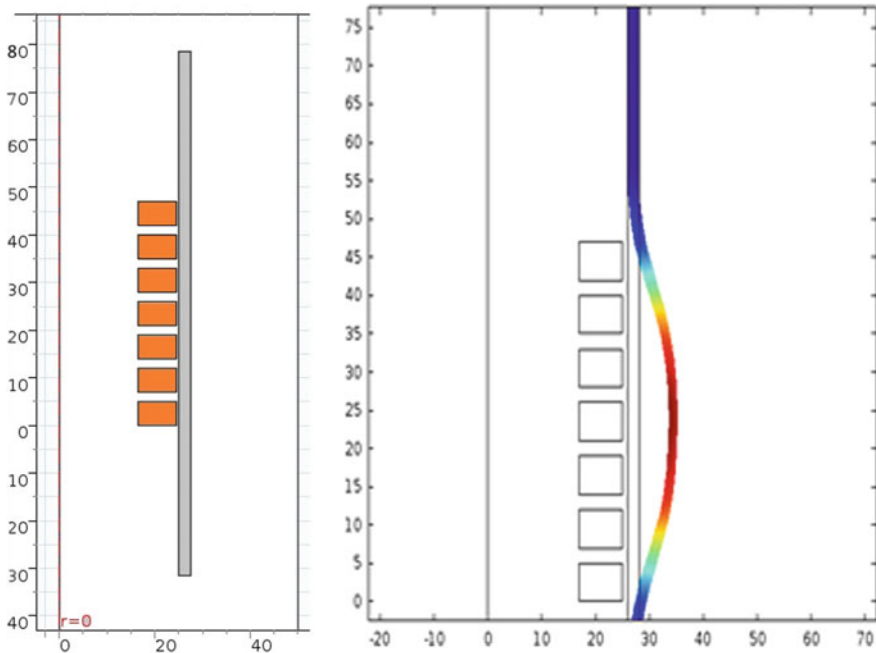


Fig. 36.7 2-D view of work-piece before and after deformation

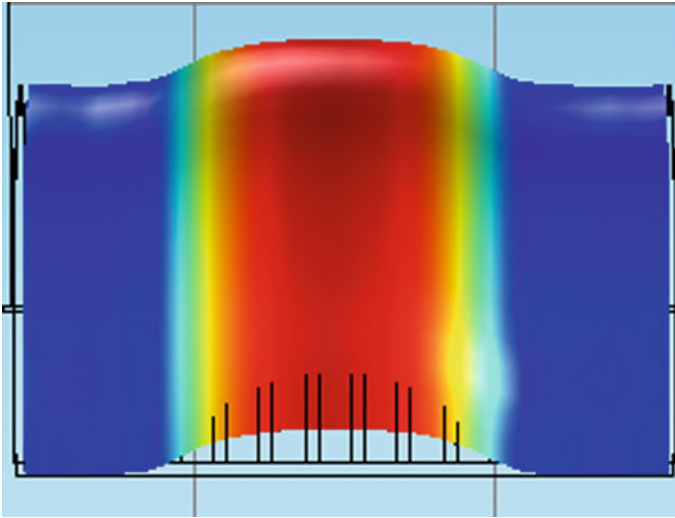


Fig. 36.8 Deformation of tube along the length of tube

The magnetic field is more concentrated at centre of the coil, as we move from the centre of coil magnetic field reduces so magnetic pressure reduces which in turn reduces deformation in longitudinal direction as shown in Fig. 36.8.

36.4 Results and Discussions

Based on the above formula, the required minimum pressure is calculated with the work-piece deformation after which the developed 2D coupled simulation model is used to evaluate displacement curve. As energy increases so the strain rate increases due to which mechanical property improves. As shown in Fig. 36.9 when charging energy increases more deformation takes place during the EMF process.

As shown in Fig. 36.9. Displacement increases with the increase in charging energy but it has not shown after work-piece so that experiment is performed. From the experiment, the result concludes that a maximum 36.2% lateral direction.

Figure 36.10 shows that pressure acts on the tube are calculated by only the analytical approach but in the sequential coupling, consider the variation of inductance and resistance and also variation in displacement. Inductance and resistance depend upon the gap between the tube and the coil. The first pick of pressure approximates the same for both analytical and sequential because during this time deformation of the tube is very small so that the inductance and resistance are the same for both the process. During the second pick of pressure deformation of the tube is considerable so that the inductance and resistance change due to which sequential pressure more drops then the analytical pressure.

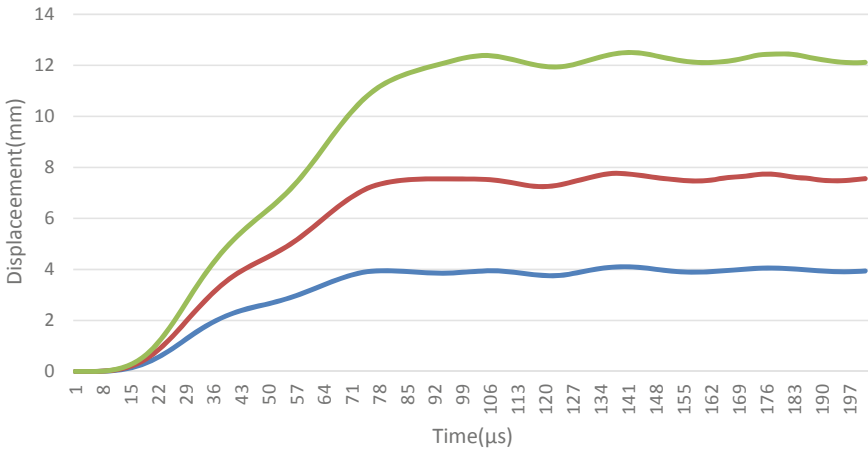


Fig. 36.9 Displacement at different charge energy (Strain rate)

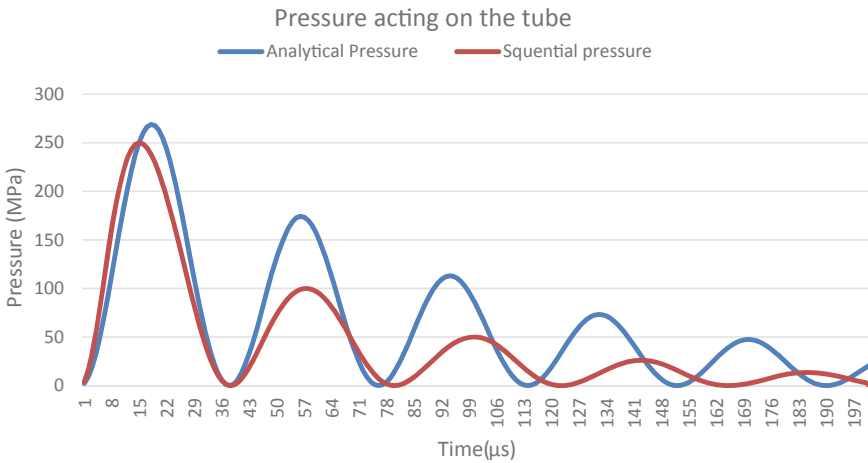


Fig. 36.10 Stress acting on the tube during the EMF process

As shown in Fig. 36.11b, stress increases with the increase in charging energy. It signifies that deformation increases with the strain rate so it shows high formability and high hardness value at a higher strain rate. Figure 36.11a shows the variation in analytical and simulation value of displacement.

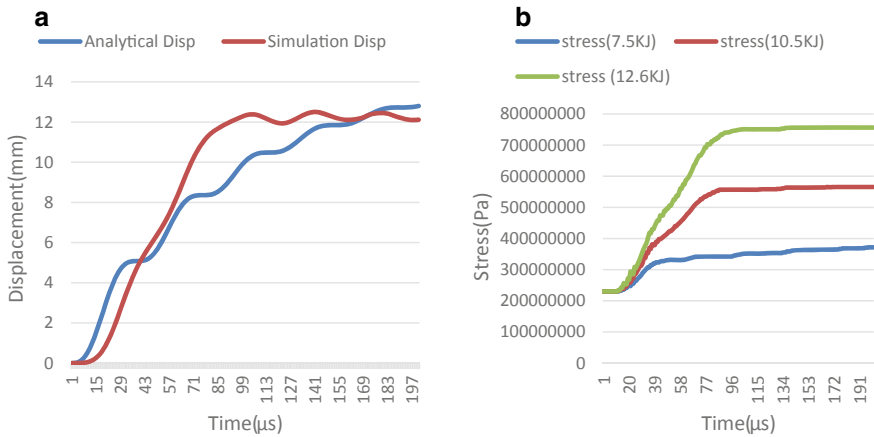


Fig. 36.11 a Comparison between analytical and simulation results b Stress versus time

36.5 Conclusions

Forming process for aluminum AA6061 is achieved at high strain rate. The following conclusions were drawn from the study:

- During the constant standard process (Low strain rate), maximum deformation in a lateral direction is 12%, and in the case of electromagnetic forming process, it increases to 36.2%.
- In the electromagnetic forming process, high strain causes huge plastic deformation which in turn increases hardness up to 58.6%.
- The percentage error in the estimated tube displacement is reduced from 19 to 5.81% in the sequential coupling.

References

1. Tian, Y., Huang, L., Ma, H., Li, J.: Establishment and comparison of four constitutive models of 5A02 aluminium alloy in high-velocity forming process. *Mater. Des.* 1980-2015 **54**, 587–597 (2014)
2. Nassiri, A., Campbell, C., Chini, G., Kinsey, B.: Analytical model and experimental validation of single turn, axi-symmetric coil for electromagnetic forming and welding. *Procedia Manuf.* **1**, 814–827 (2015)
3. Dond, S., Choudhary, H., Kolge, T., Sharma, A.: Analysis of the variation of the discharge circuit parameters during electromagnetic forming processes. *Int. J. Precis. Eng. Manuf.* **20**(3), 375–382 (2019)
4. Dond, S., Choudhary, H., Kolge, T., Sharma, A., Dey, G.K.: Robust electromagnet design for pulse forming application. *COMPEL - Int. J. Comput. Math. Electr. Electron. Eng.* COMPEL-05-2018-0229 (2019)

5. Kore, S.D., Date, P.P., Kulkarni, S.V.: Effect of process parameters on electromagnetic impact welding of aluminum sheets. *Int. J. Impact Eng* **34**(8), 1327–1341 (2007)
6. Doley, J.K., Kore, S.D.: Electromagnetic formability of an aluminium ice tray. *Key Eng. Mater.* **611–612**, 1124–1131 (2014)
7. Psyk, V., Risch, D., Kinsey, B.L., Tekkaya, A.E., Kleiner, M.: Electromagnetic forming—a review. *J. Mater. Process. Technol.* **211**(5), 787–829 (2011)
8. Kleiner, M., Beerwald, C., Homberg, W.: Analysis of process parameters and forming mechanisms within the electromagnetic forming process. *CIRP Ann.* **54**(1), 225–228 (2005)